CrossMark

Activated Carbon-Coated Electrode and Insulating Partition for Improved Dust Removal Performance in Electrostatic Precipitators

Kwang-Soo Kim · Sungyoun Kim · Tae Hwan Jun

Abstract The dust removal performance of two types of modified electrode electrostatic precipitator systems was evaluated and compared with that of a conventional aluminum plate electrode using laboratory-scale experiments. In the novel electrode systems, the electrode surface was coated with activated carbon using a mixed slurry containing carbon black, polyvinyl acetate, and methanol. The modification of the electrode surface improved dust precipitation by increasing the specific capacitance of the electrode. The modification also lowered the electrode's resistance and increased its specific surface area. The optimum electrode spacing and electric voltage supply were determined using batch-type tests. In addition, dielectric insulators were applied as a partition between the oppositely charged electrodes equipped with the modified electrode plates. Multi-layered office paper cut to the same size as the electrodes was used as an insulating material. The addition of the insulator resulted in excellent improvement in the dust removal performance by minimizing the back-corona discharge phenomenon as well as doubling the dust collecting surface. Continuous dust removal tests with the three electrode systems revealed that whereas the conventional aluminum electrode exhibited 54 % dust removal, the activated carbon (AC)-coated system showed 85 % and AC-coated + insulator system showed 90 % and higher dust removal efficiency.

Keywords Electrostatic precipitator · Activated carbon · Dielectric characteristics · Insulator · Dust removal

K.-S. Kim · S. Kim
Environmental and Plant Engineering Research Institute, Korea Institute of Civil Engineering and Building Technology, 283 Goyang-daero, Ilsanseo-gu, Goyang-si, Gyeonggi-do 10223, Republic of Korea

S. Kim
e-mail: sykim1202@kict.re.kr

K.-S. Kim (✉) · T. H. Jun
Department of Construction Environment Engineering, University of Science and Technology Korea, 217 Gajeong-ro, Yuseong-gu, Daejeon 34113, Republic of Korea
e-mail: kskim@kict.re.kr

T. H. Jun
e-mail: hotbear17@nate.com

1 Introduction

Electrostatic precipitators (ESPs) are widely used in particulate collection, especially in industrial complexes that generate large volumes of contaminated air. In ESP systems, dust particles are removed mainly by the force of an induced electrostatic attraction as they flow through the device in an air stream. Typical ESPs operate basically by three steps: corona discharge to dust particles in flowing air, precipitation of charged particles to the collecting electrodes, and cleaning of the particles from the electrode (White 1963). In corona discharge, the electrode emits a strong electrical field that charges dust particles in the surrounding air. The charged particles are attracted and become attached to collecting electrodes (Yamamoto and Velkoff 1981; Mizuno 2000). Problems associated with this process include

high electrical power consumption and the production of toxic ozone and NO_x gases from the oxygen and nitrogen in the air (Rehbein and Cooray 2001). Additionally, as dust particles stack on the collecting electrode, re-entrainment of the particles occurs, and thus, the removal efficiency deteriorates with the passage of time. Particle re-entrainment is observed when the gas velocity exceeds an acceptable level or when uniform velocity and electrical power distribution are lost. Problems also can be generated during the rapping process or because of back corona. Back-corona discharge is a well-known phenomenon aroused by a series of micro-discharges in the air between the particles of the dust layer deposited on the collecting plates. It is initiated when the particle resistivity becomes quite high and tends to neutralize the particle charge and change the voltage–current characteristics of the system. All of these processes result in significant deterioration in the removal efficiency (Chang and Bai 1999; Bacchiega et al. 2006). Another consequence of back corona is that the corresponding lowering of spark-over voltage and increased discharge current result in high energy consumption (Jaworek et al. 2007).

Attempts to overcome the above concerns and associated issues to improve dust collection efficiency have been made in many studies, including control of operational temperature (Noda and Makino 2010), application of bipolar corona discharge (Katatani et al. 2012; Xiang et al. 2001), and changing the electrode configuration and energization (Canadas et al. 1997; Mizuno 2000). Kearns (1979) enhanced particle charging in the corona discharge field by adopting a high velocity ionization stage, which provided operating field strengths of 10–17 kV/cm, compared with 3–6 kV/cm in a conventional ESP, and gas velocities 7–10 times higher than those used in conventional ESP systems. Low and uniform current densities at the collecting electrodes were achieved using small barb distances and small discharge electrode distance by Miller et al. (1998), suggesting that changing the electrode configuration can improve fine dust removal efficiency as well as reduce negative effects like the back-corona phenomenon. Kuroda et al. (2003) observed an increased discharge current by modifying the shape of the electrodes with punched holes. Comparing a typical plane electrode with punched electrodes of three hole sizes, they found that the collection efficiency was highest for the electrode with 3.1-mm-sized holes. Recently, attempts to improve electric field conditions have been made by changing the electrode

material from typical metals to non-metal carbon sheets. Kim et al. (2011) developed an anticorrosive ESP system equipped with carbon graphite discharger and PVC sheets with metal insert as collection plates and obtained a strong collection performance of 95 % for ultrafine particles with low energy consumption.

The present authors suggested (Kim et al. (2013)) the use of activated carbon as a coating for metal electrode surfaces to make electrodes with improved conductivity and electrosorption capacity. Activated carbon (AC) has been used in electrode fabrication in many ways, as a tool to increase specific capacitance, lower resistance, and increase specific surface area. In the form of double layer capacitors, AC has demonstrated excellent performance as a high power density electrode in a variety of applications (Osaka et al. 1999; Gamby et al. 2001; Portet et al. 2005; Zou et al. 2008). AC-coated electrodes (Kim et al. 2013) applied to simultaneous removal of dust and gaseous contaminants have exhibited as high as 90 % dust (3000–4000 $\mu g/m^3$) and gas (NH_3 and H_2S) removal even with no corona discharge step, attributed to the increased electrical charge density. Thus, the desired dust collection efficiency was achieved without corona discharge and with high energy efficiency while preventing the generation of ozone and NO_x.

In this study, AC-coated electrodes were evaluated with laboratory-scale continuous dust removal experiments and compared with a typical aluminum electrode. Parallel electrode geometry was used to enhance the dust plate contact surface to optimize dust collection efficiency at relatively high air flow rate. In addition, insulating panels were applied between oppositely charged electrodes to ease the interference between the charged particles. The panels act to separate the opposing electric fields so that the charged particles are collected on the oppositely charged electrode surface without the interference of other particles or the adjacent oppositely charged electrode, which should help minimize back discharge effect. Therefore, this study aims to improve conventional ESP systems by improving the capacitance, resistance, and surface area of the electrodes using an AC coating to collect particulate matter at higher efficiency. In addition, application of insulating panels between electrode plates was expected to improve the dust collection efficiency by minimizing back discharge phenomena. Continuous lab-

scale dust removal tests were conducted with a typical metal electrode system, AC-coated electrode system, and AC-coated and insulating panel system to evaluate the effects of the modifications on dust removal performance.

2 Experimental Methods

2.1 Design of the AC-Coated ESP System

Electrode plates were coated with an activated carbon powder paste containing AC, carbon black (CB), polyvinyl acetate (PVAc), and methanol. The AC powder was washed with boiling water several times, with boiling 1 N HCl, and then washed again with water and dried before use. The acid-treated AC was mixed with carbon black to reduce electrical resistance (Nadakatti et al. 2011), and PVAc was added to bind the coating to the electrode surface. Methanol was added to ensure dispersion of the three ingredients and allow the application of an even coating onto the electrode surface. The optimum ratio of the components was found in previous research (Kim et al. 2013) to be 10 g:2 g:3 g:20 mL of AC/BC/PVA/MeOH. The AC mixture was spread on the aluminum electrode surface, and the electrode was placed in a 100 °C oven to remove the methanol. The Brunauer–Emmett–Teller (BET) surface areas of the coated AC and original powdered AC were determined by nitrogen adsorption method at 77 K, using automatic high-end volumetric gas adsorption instrument (BELSORP-max, MicrotracBEL Corp, Osaka, Japan). The obtained AC-coated electrode plates were then used in continuous dust removal tests.

2.2 Determination of Optimum Electrode Distance and Electric Voltage Supply

Using the AC-coated electrode, three different distances between electrode plates were tested with a fixed dust loading rate and electric voltage supply. The electrodes were placed at 3-, 2-, and 1-cm intervals. The dust concentrations in and out of the device were monitored, and the amount of particulates collected on the plate was weighed. The optimum electric voltage supply was investigated by applying 0, 3, 5, 7, and 9 kV to the AC-coated electrode system under the fixed dust loading condition.

### 2.3 Application of Insulators Between AC Electrodes

Among the various potential insulating materials, common office paper was chosen to be used as the partition between AC-coated electrodes. The paper was cut to the same size as the electrodes and stiffened with PVAc in the form of multiple adhered layers. The resulting paper plates were then applied to the electrodes, and their effect on dust removal was tested.

2.4 Continuous Dust Removal Experiment

The experiment was performed in a lab-scale dust control chamber as shown in Fig. 1. The dust control system was an electrode plate precipitator consisting of a dust generator (fluidized bed dust generator, Model 3211, Kanomax, Osaka, Japan), blower, dust mixing tank, electrostatic precipitation chamber with electrode plates, electric voltage supplier, and dust counters (dust monitor, Model 3442, Kanomax). Air containing dust from the dust generator at a fixed relative humidity of approximately 25 % was made to flow through a pressure regulator adjusted to a fixed flow rate of 6.7 cm/s (90 L/min) for all experiments. The dust collecting chamber consisted of four sequential cells, each of which contained 11 electrodes installed at 10-mm intervals. The electrodes were connected alternately to the anode and cathode by an electric wire to the voltage supplier.

In advance to the artificial dust that was applied, air flow distribution in the chamber was determined using air velocity meter (TSI-9515 VelociCheck, Naraetek, Pusan, Korea). Under 90 L/min air flow condition, the flow rate was monitored at the center and the four corners of the chamber, and the difference in the measured flow rates was found ±0.4 %. In this experiment, it was regarded that discrepancy in the flow rate was not great; therefore, the monitoring of dust concentration was only conducted at the center.

Reagent grade JIS test powder (Test Powder 1, class 11) was used as a PM10 dust and supplied through the dust generator. The particle size of the powder was within 0.3–5 μm. The chemical composition of the powder was SiO_2 (34–40 %), Fe_2O_3 (17–23 %), Al_2O_3 (26–32 %), CaO (0–3 %), MgO (0–7 %), and TiO_2 (0–4 %). Dust counters were equipped in the dust control chamber to monitor the numbers of dust particles before and after
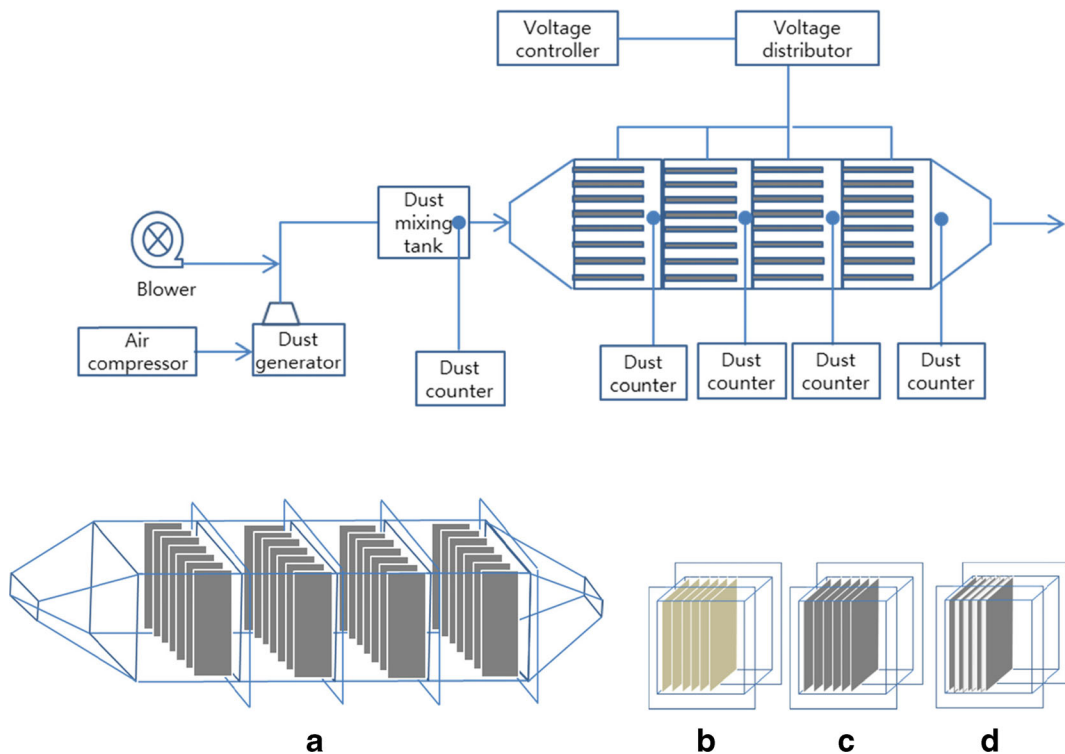
Fig. 1 Schematics of electrostatic precipitator system with electrode configuration and arrangement: **a** dust control chamber with AC-coated electrodes, **b** aluminum electrode, **c** AC-coated electrode, and **d** AC-coated electrode and stiffened paper plate as an insulator in turn

precipitation. All experiments were conducted at room temperature, about 20 °C.

The continuous dust removal test was conducted with three different electrode systems: one with typical aluminum electrode plates, one with AC-coated electrode plates, and one with AC-coated electrode plates and stiffened office paper plates. Figure 1 shows a schematic of the system with individual electrodes installed (Fig. 1b–d), whereas Table 1 lists the specifications of the dust removal systems and their operating conditions.

3 Results and Discussion

3.1 Comparison of BET Surface Area

Activated carbon powder was uniformly coated on the aluminum electrode surface so that the resulting uniform electric density would cause dust particles to evenly precipitate on the electrode surface. Carbon black was added to the coating material to improve electric conductivity. To achieve the expected result, it was important that the AC coating had a high porosity and that its

Table 1 Dust removal system specification and operational conditions

	Typical metal electrode	Modified electrode	
Electrode material	Aluminum	Aluminum coated with AC	Aluminum coated with AC and stiffened paper (insulator)
Plate spacing (mm)	10	10	5 (electrodes and insulators in turn)
Plate size (H × L) (mm^2)	145×45	145×45	145×45
Number of plate	44	44	44 (electrode) + 44 (insulators)
Voltage supplied	5 kV	5 kV	5 kV
Gas velocity	6.67 cm/s	6.67 cm/s	6.67 cm/s

surface area was kept intact. Any material added as a binder may block the pores of the AC. The optimal mixing ratio of AC, CB, PVAc, and methanol and the best drying method were found in our previous research (Kim et al. 2013). The PVAc functioned as a glue to bind the AC powder to the electrode surface, while methanol was added to prevent the thickening of the mixture. A prepared and dried AC coating was detached from an electrode for BET surface area measurements, which were compared with those of the original AC powder (Table 2).

As listed in Table 2, the BET surface area of the original AC powder was decreased by 54 % after it was mixed with the other coating materials. The pore volume also showed a similar decrease (0.33 to 0.19 cm^3/g). It was found that PVAc had the greatest effect on the surface area of the coating, whereas the CB and methanol did not seem to significantly influence the pore surface. The addition of methanol not only allowed the AC paste to be coated uniformly on the electrode surface but also helped to open the pores of the AC as it evaporated from the inside of the pores when the coating was dried in the oven. Figure 2 shows images of the aluminum electrode plates before and after AC coating.

3.2 Optimum Electrode–Electrode Distance and Electric Voltage Supply

The patterns of dust collection and the dust removal efficiency of the electrode system can differ depending on the parameters of the system. Preliminary tests were carried out to determine the most appropriate electrode spacing and electric voltage supply to optimize dust removal performance. For 30-mm electrode spacing, four AC electrode plates were installed in the dust collecting chamber and operated for 10 h, receiving a total dust mount of approximately 10 mg/m^3. Every 1 or 2 h, the electrode with the highest deposited dust density was removed from the system and weighed and then
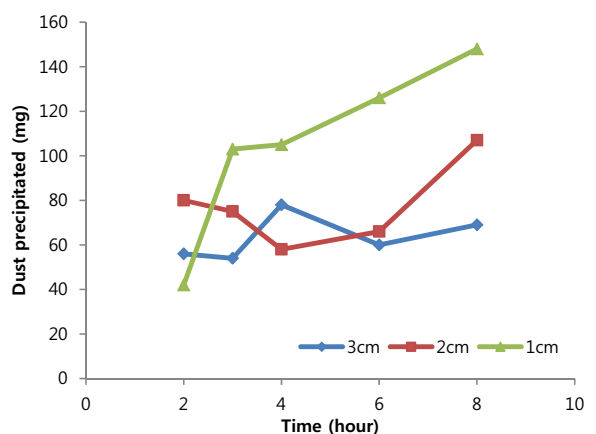

Fig. 2 Aluminum electrode before and after AC coating

reinstalled to continue the experiment. For 20-mm electrode spacing, six AC electrode plates were installed and operated in the same manner. For 10-mm electrode spacing, eight AC electrode plates were installed. Figure 3 illustrates the results of the electrode spacing experiment. Because the plot shows the amount of dust collected by only one electrode plate in each test, it does not necessarily show the efficiency of the entire system. Dust removal increased proportionally with the passage of time only in the system with 10-mm spacing, whereas for the other two spacings, the dust removal was unstable and showed a fluctuating pattern. It is understood that the narrower the electrode spacing, the higher the current density at the same supplied voltage. This is

Table 2 BET surface area

Coating mixture	BET surface
Activated carbon (AC)	1144 m^2/g (0.33 cm^3/g)
Carbon black (CB)	31 m^2/g
AC + methanol	1128 m^2/g
AC + PVAc	481 m^2/g
AC + BC + PVAc + MeOH	529 m^2/g (0.19 cm^3/g)

Fig. 3 Time passage dust removal performance according to electrode–electrode distance

clearly shown by the result that the highest dust collection was obtained in the AC-coated electrode system with an electrode spacing of 10 mm.

Figure 4 shows the results obtained with application of increasing electric voltage. For each electrode spacing condition, four levels of electric voltage were supplied and without voltage supply (0 V) as a control were tested for dust removal performance. At 20-mm electrode spacing, dust precipitation increased with voltage supply, but at wider electrode spacing, it seemed that the dust layer became detached from the plate at high voltage supply, and at narrow spacing, little correlation was found between voltage supply and dust removal at 5 kV and above. As mentioned before, a back discharge effect often occurs in systems with wider electrode spacing and at high voltage conditions if the electrode–electrode space is narrow. Overall, dust removal was best when 10-mm electrode spacing was used, and in this case, a voltage supply of 5 kV was found to be most beneficial. Following continuous dust removal tests were therefore conducted with 10-mm electrode spacing and at 5 kV.

3.3 Continuous Dust Removal Tests

The continuous dust removal performance of the three fabricated types of electrode systems was evaluated. First, 11 typical aluminum plate electrodes were equipped alongside in a cell, and four cells were connected lengthwise. Therefore, the dust removal chamber contained total 44 electrode plates and received airflow containing particulate matter at 90 L/m (6.67 cm/s) flow rate. The second system contained AC-coated electrodes instead of aluminum electrodes, and the third system contained 44 insulator plates, made of stiffened office
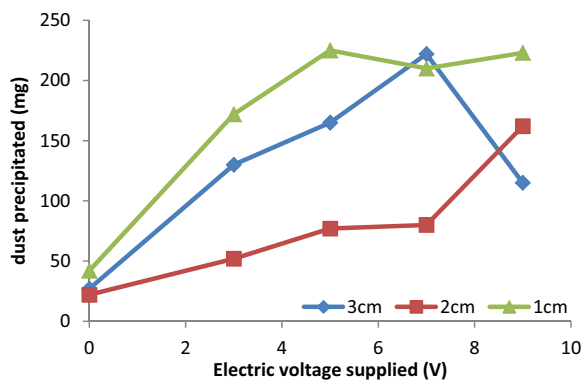
Fig. 4 Dust removed by increasing electric voltage supplied at different electrode–electrode distance

paper with PVAc as glue, in addition to the 44 AC-coated electrodes. In this case, the electrode spacing became even narrower, 5 mm, whereas the former two systems had an electrode spacing of 10 mm.

Dust concentrations were monitored in the dust mixing tank for the influent, port 1 after the first set of 11 electrodes in the first cell, port 2 after the second set of electrodes in the second cell, port 3 after the third set of electrodes in the third sell, and port 4, the effluent after treatment by the entire system. Besides the dust concentration monitoring, each electrode plate was weighed before and after the experiment to determine the dust removal pattern within the chamber. The dust monitoring results are shown in Fig. 5, in the order of aluminum plate (a), AC coating (b), and AC coating + insulator (c) systems. Although the influent dust concentration was controlled by the fluidized dust generator (Model 3211, Kanomax) during the experiment, the mean influent dust level in each experiment varied more and less; as 7.31 mg/m^3 ($\pm$1.67) in aluminum electrode system (a), 10.80 mg/m^3 ($\pm$1.28) in AC-coated electrode system (b), and 12.68 mg/m^3 ($\pm$2.43) in AC + insulator system (c).

The tests were carried out for approximately 400 min. In the case of the typical aluminum electrode cell, it was observed that the entering particulate matter was collected in an orderly fashion as the air stream moved through the cells. For the first 200 min, cell 1 removed the largest portion of dust but afterwards, cell 2 appeared to collect more dust. Cells 3 and 4 did not contribute much to the performance of the system. In this system, dust precipitation became unstable as the deposited particulates built up on the electrodes with time, and the concentration of particulates in the effluent (port 4) increased gradually.

The same experiment was conducted with AC-coated electrodes instead of aluminum plate. The dust removal performance started quite stable and satisfactory, with all four cells contributing to the removal efficiency of the system. It appeared that more than 40 % of entering particulates were captured in the first cell, half of the remaining particulates were captured in cell 2, and the other two cells collected the last evenly. This pattern of dust removal continued for a fairly long time during the experiment, but the removal efficiency of cell 1 gradually deteriorated with particulate build up.

The dust removal efficiency of the system containing AC-coated electrodes and insulating plates was even better, and the system exhibited good and stable effluent
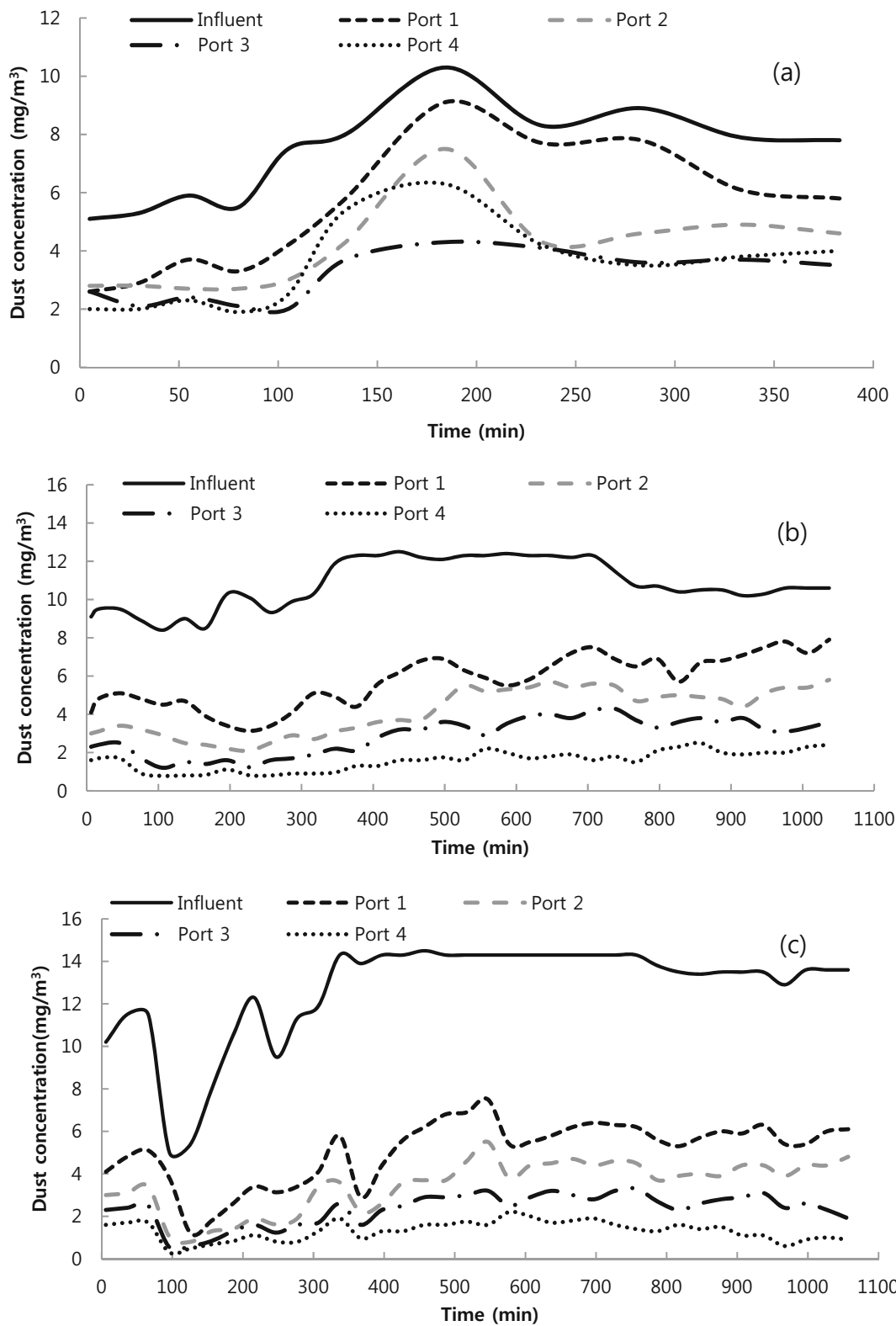
Fig. 5 Comparison in dust removal performances between **a** conventional aluminum electrode, **b** AC-coated electrode, and **c** AC + insulator system

quality. As expected, about half of the entering particulate matter was collected in cell 1, but the other three cells also contributed evenly to the removal of the remaining dust, especially during the last half of the experiment. Unlike the other two systems, the dust removal performance became better and constant with time, likely the result of successful interruption of the back discharge effect by the insulating plates applied between the electrodes.

Figures 6, 7, and 8 show the mass of dust distribution collected on the surfaces of the electrodes after operation of each system. The electrode plates were removed from the dust collection chamber and weighed for comparison with their weights before the experiment. Figure 6 shows the results obtained for the aluminum electrode system after 383-min operation. Along with the air flow shape, it is clear that more particulate matter was captured in the center of the cell and less was captured at the outer sides. In cell 1, more dust was collected on the electrodes at odd-numbered position, which were connected to the anode (+). The systems in this study remove dust particles without corona discharge but by exploiting each the natural charge characteristics of each particle. Thus, the greater amounts of dust collected by the odd-numbered electrodes were because the dust particles were more negatively (−) charged. Nevertheless, a high number of particles also precipitated on the cathode electrodes, because dust particles naturally have either (+) or (−) charge and this can be easily switched by any external stimulation. Because most (−) charged particles were removed in cell 1, more (+) charged particles remained and collected on even-numbered electrodes (connected to the cathode (−)) in cell 2. This trend is clearly observed for cell 3 as well as cell 4.

Figure 7 shows the results for the AC-coated electrode system. This system was operated at high efficiency for a long time, 1080 min. As observed in Fig. 6, more dust was collected in the first cells and at the central electrode positions. Reflecting the longer operation time as well as the modification of the electrode surface, the maximum mass of dust collected by a single electrode was 794 mg, compared with 222 mg for the Al electrode system. It is notable that in cell 1, more dust collection took place on the electrodes at even-numbered positions which were connected to the cathode (−), than on those at odd-numbered positions. As mentioned above, dust particles naturally have either (−) or (+) charges, and it seems that (−) charged particles are

not always dominant in number. This time, more particles were collected on cathode first, and the opposite was in the following cells.

Figure 8 shows the dust removal observed for the system with alternately positioned AC-coated electrodes and stiffened paper insulating material. Like the previous tests, the entering particulates were mostly precipitated in the front set of electrodes (cell 1) and distributed more in the center. More particulates were collected by the odd-numbered electrodes, i.e., anodes, in cell 1, following the same trend as that observed for the aluminum electrode system. Interestingly, a high mass of particulate precipitated on the paper, which was applied to diminish possible back discharge effects. As electrodes become stacked with dust, back-corona discharge can be formed between the dust particles and the electrode, causing an increase in the particle resistivity and finally particle re-entrainment. Physically blocking between each pair of electrodes with an insulating material was expected to reduce charge interference between particles and between particles stacked on the top of the layer and the electrode next to it. Although the paper plates physically blocked the electric field between pairs of electrodes, they also functioned as a dielectric dust collector despite not being directly connected to the electric supply. Placed between the high current density electrodes, the paper naturally displayed dielectric properties and therefore contributed to the dust collection even more than the electrode plates. This effect is clearly shown in the cells 2–4, in which the insulators had a greater part in dust removal than the electrodes.

The efficiency of dust collection in ESPs can be estimated by simple Deutsch–Anderson equation (Eq. 1), which has been used widely to determine precipitator performance in ideal conditions. This was modified by Matts and Ohnfeldt (Eq. 2), to account for non-ideal effects (Chang et al. 1995). In Deutsch–Anderson equation, ESP efficiency is predicted with the assumption that particle size and its migration velocity are uniform, and so is the flow rate in the entire ESP system. Because this is not true in a real precipitator condition, the term "average migration velocity (W_k)" and the constant "k" were added in the Matts and Ohnfeldt equation. The three types of electrode system performances were evaluated with the equations, and the results are summarized in Table 3.

Fig. 6 Dust removed in aluminum electrode system
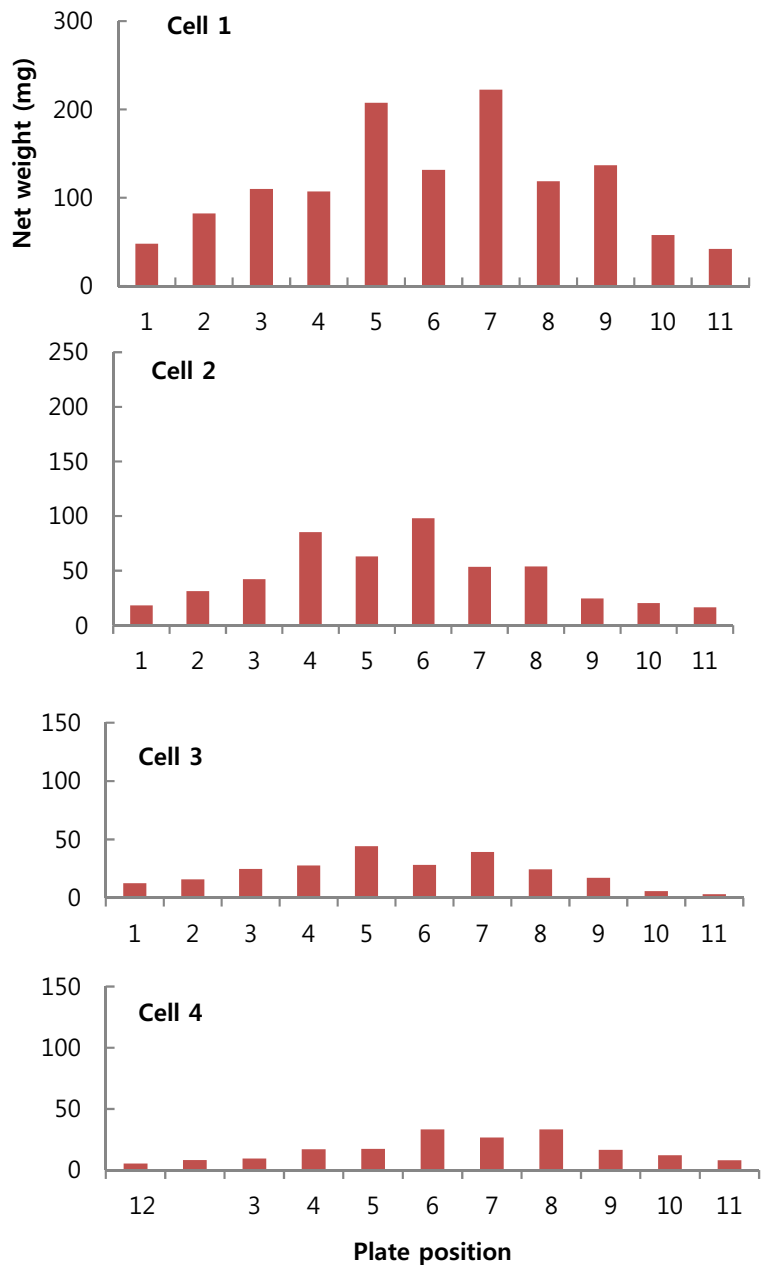
$$\eta = 1 - \exp\left(-W \cdot A / Q\right) \qquad (1)$$

$$\eta = 1 - \exp\left[-W_k\left(A / Q\right)^k\right] \qquad (2)$$

in which η is the collection efficiency of the precipitator, W is the migration velocity (m/s), A is the effective collection area (m^2), and Q is the gas flow through the precipitator (m^3/s). The term W_k in Matts and Ohnfeldt equation is averaged migration velocity. The constant k is usually between 0.4 and 0.6, depending on the variation of particle size and other dust properties. In this study, Metts–Ohnfeldt equation was found best to simulate the experimental result, especially when the constant k was 0.5. In the aluminum electrode system

Fig. 7 Dust removed in AC electrode system
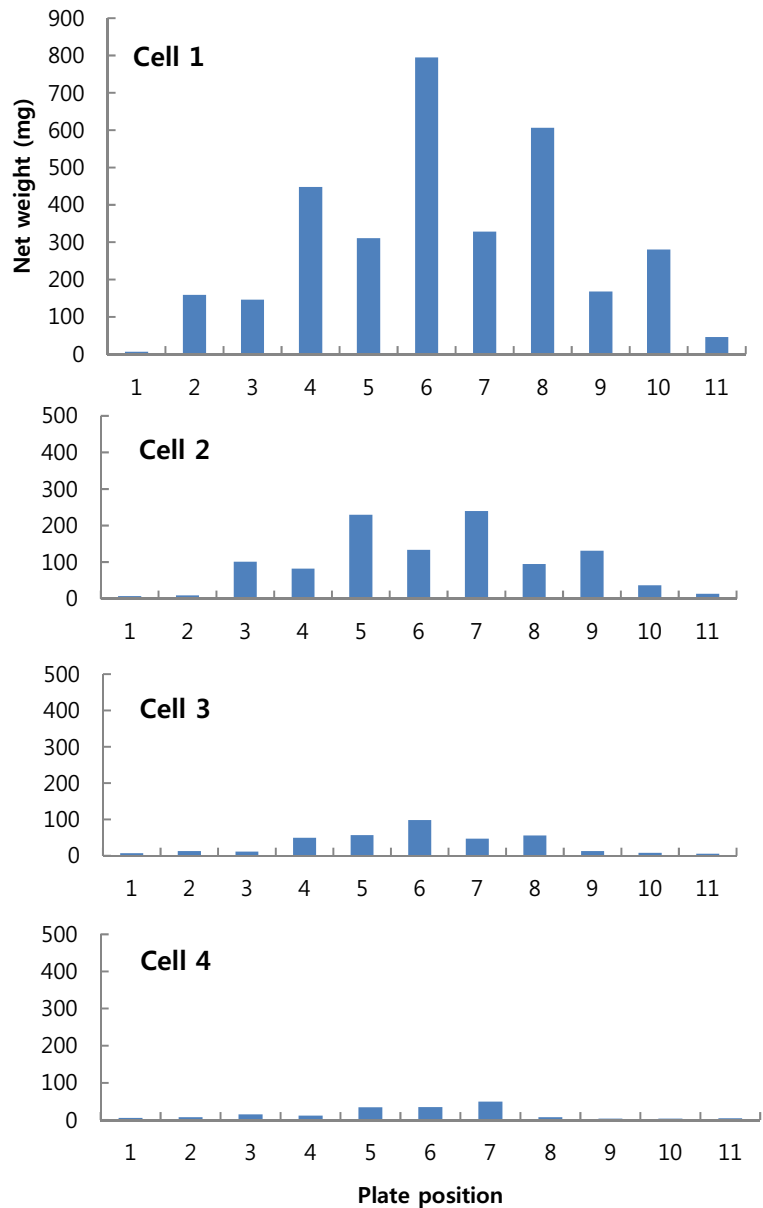
however, k value of 0.4 was the best fit. The equation should be used efficiently to estimate collection surface area required to meet satisfactory dust collection efficiency.

The mean dust removal efficiencies of the individual systems measured at each sampling port are illustrated in Fig. 9 and quantitatively summarized in Table 3. Dust collection performance clearly improved in the order typical aluminum electrode system > AC-coated electrode > AC + insulator.

Coating the aluminum electrode surfaces with AC increased the dust removal efficiency by 57 %, and the efficiency was improved even more (65 %) with insulator application. The application of insulating material appeared to display a good synergistic effect, improving the dust precipitation performance by blocking back-corona discharge and themselves collecting particulate matter. The dielectric characteristics of the material should have an important role in its efficiency, because the material

Fig. 8 Dust removed in AC + insulator system
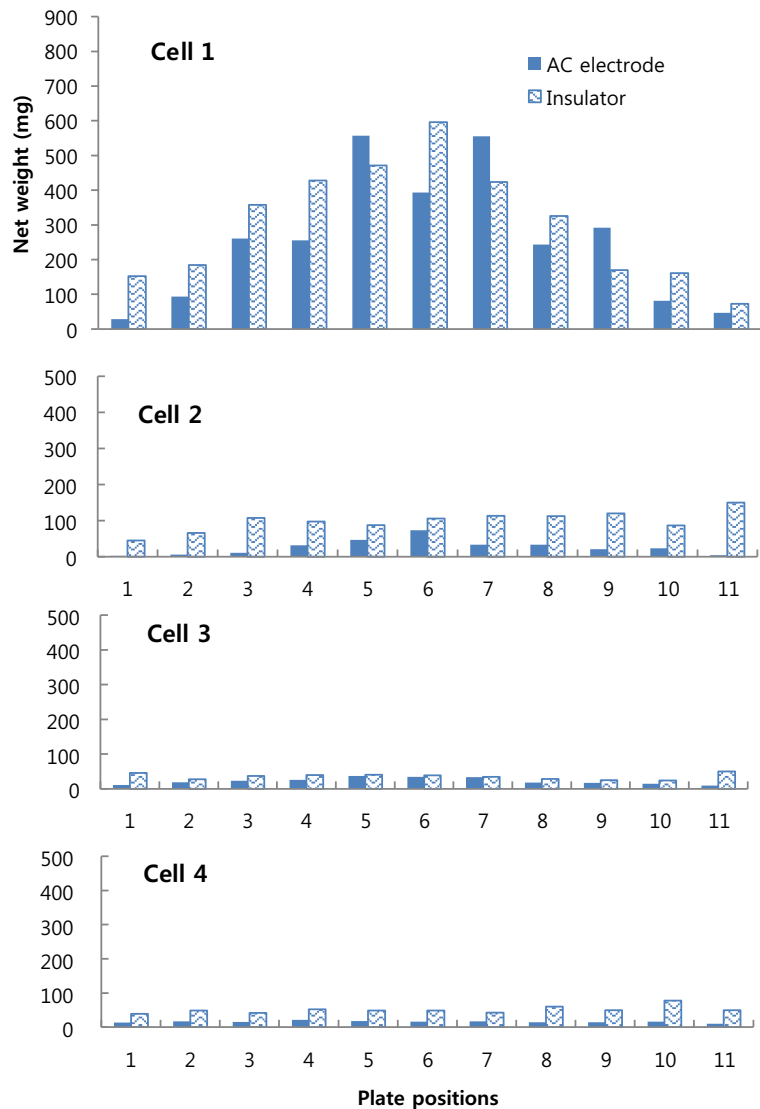
functioned as a collecting electrode without a power supply. Further study should investigate the use of different dielectric materials which have both high dielectric constant and safety in practical application.

4 Conclusion

In this study, two laboratory-scale-modified electrostatic precipitators were designed and evaluated for dust control. Excellent improvement in removal efficiency was obtained compared with that of a conventional system. The surface of typical aluminum electrodes were coated with an activated carbon paste in the form of a mixture with carbon black, PVAc, and methanol. The high specific surface area AC coating increased the specific capacitance and lowered the resistance of the electrode. This effect was clearly proven through the continuous dust removal test, which showed a 31 % increase in the removal efficiency compared with that of the typical aluminum electrode system. Back-corona discharge is a common phenomenon that reduces collection efficiency, and it was successfully controlled in this study by the application

Table 3 Estimations of dust removal efficiency (%) using the Deutsch–Anderson and Metts–Ohnfeldt equations

		Deutsch–Anderson eq.	Metts–Ohnfeldt eq.			This study
	Distance from inlet	$k=1$	$k=0.4$	$k=0.5$	$k=0.6$	
Typical (Al) electrode	1	99.83	33.87	47.93	64.29	29.3 (±14.7)
	2	99.99	42.05	60.26	79.00	46.0 (±8.6)
	3	100	47.36	67.70	86.34	57.7 (±6.7)
	4	100	51.32	72.88	90.61	54.4 (±11.2)
AC-coating electrode	1	99.83	33.87	47.93	64.29	46.6 (±11.3)
	2	99.99	42.05	60.26	79.00	61.9 (±9.5)
	3	100	47.36	67.70	86.34	73.8 (±7.5)
	4	100	51.32	72.88	90.61	85.4 (±4.6)
AC coating + insulator	1	99.99	42.05	60.26	79.00	60.0 (±9.9)
	2	100	51.32	72.88	90.61	73.3 (±6.7)
	3	100	57.12	79.78	95.11	82.0 (±3.9)
	4	100	61.33	84.21	97.23	89.8 (±2.8)

of insulating material between the electrode plates in the dust collecting chamber. Multiple-layered paper plates of the same size as the electrode plates were used as a dielectric insulator. Placed in between the electrodes, the insulating material blocked the interference of charged particles with other particles and also with other electrode plates of opposite charge. At the same time, the dielectric property of the material allowed it to function as a collecting electrode for dust entering the chamber. Application of the modified Deutsch–Anderson equation revealed that the dust removal efficiency

could be predicted by the Metts–Ohnfeldt equation especially with the k value of 0.5. The experimental results showed that the insulator plates collected an even greater mass of the particulate matter than the collecting electrodes in the same cell. The total dust mass collected by the AC-coated electrodes was 3502 mg, whereas the insulators collected 5377 mg. Unsurprisingly, this novel system with AC electrode and insulating material exhibited the best dust removal performance among the three tested systems. Further studies should investigate the application of insulating materials with higher

Fig. 9 Mean dust removal efficiencies in individual systems
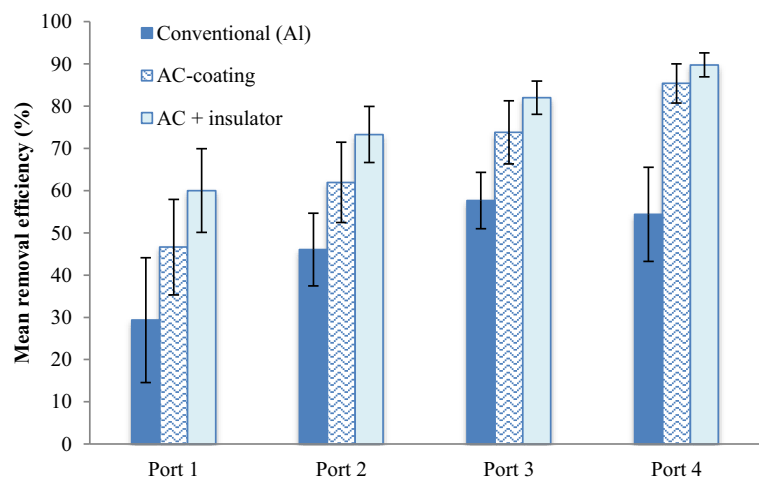
dielectric properties but assured safety for practical applications at the same time.

Conflict of Interest   The authors declare that they have no conflict of interest.

References

Bacchiega, G., Gallimberti, I., Arrondel, V., Caraman, N., & Hamil, M. (2006). *Back-corona model for prediction of ESP efficiency and voltage–current characteristics.* X International Conference on Electrostatic Precipitation (ICESP X), Cairns, Queensland, Australia Paper 3 B3.

Canadas, L., Navarrete, B., Ollero, P., & Salvador, L. (1997). Parametric testing of coal electrostatic precipitator performance. *Environmental Progress, 16*(2), 98–105.

Chang, C., & Bai, H. (1999). An experimental study on the performances of a single discharge wire-plate electrostatic precipitator with back corona. *A. Aerosol. Sci., 30*(3), 325–340.

Chang, J., Kelly, A. J., & Crowley, J. M. (1995). "*Handbook of electrostatic processes*". New York: Marcel Dekker, Inc.

Gamby, J., Taberna, P. L., Simon, P., Fauvarque, J. F., & Chesneau, M. (2001). Studies and characterizations of various activated carbons used for carbon/carbon supercapacitors. *Journal of Power Sources, 101*, 109–116.

Jaworek, A., Krupa, A., & Czech, T. (2007). Modern electrostatic devices and methods for exhaust gas cleaning: a brief review. *J. of Electrostatics, 65*, 133–155.

Katatani, A., Hosono, H., Murata, H., & Mizuno, A. (2012). Collection performance of an electrostatic precipitator using bipolar corona discharges. *Proceedings of the 2012 Electrostatic Joint Conference*. Cambridge, ON, Canada, June 12–14, ESA2012 e-proceedings S36, 1-5.

Kearns, M. T. (1979). High intensity ionisation applied to venture scrubbing. *J. Air Pollut. Control Assoc., 24*(4), 383–385.

Kim, K. S., Park, J. O., Lee, J. H., Jun, T. H., & Kim, I. H. (2013). Simultaneous removal of gas and dust by activated carbon coated electrode. *Environ. Eng. Res., 18*(4), 229–234.

Kim, H., Han, B., Kim, Y., Hwangm, K., Oh, W., Yoo, S., & Oda, T. (2011). Fine particle removal performance of a two-stage wet electrostatic precipitator using a nonmetallic pre-charger. *J. Air Waste Manag. Assoc., 61*(12), 1334–1343.

Kuroda, Y., Kawada, Y., Takahashi, T., Ehara, Y., Ito, T., Zukeran, A., Kono, Y., & Yasumoto, K. (2003). Effect of electrode shape on discharge current and performance with barrier discharge type electrostatic precipitator. *Journal of Electrostatics, 57*, 407–415.

Miller, J., Hoferer, B., & Schwab, A. J. (1998). The impact of corona electrode configuration on electrostatic precipitator performance. *Journal of Electrostatics, 44*, 67–75.

Mizuno, A. (2000). Electrostatic precipitation. *IEEE Transactions on Dielectrics and Electrical Insulation, 7*(5), 615–624.

Nadakatti, S., Tendulkar, M., & Kada, M. (2011). Use of mesoporous conductive carbon black to enhance performance of activated carbon electrodes in capacitive deionization technology. *Desalination, 268*, 182–188.

Noda, N., & Makino, H. (2010). Influence of operating temperature on performance of electrostatic precipitator for pulverized coal combustion boiler. *Advanced Powder Technology, 21*, 495–499.

Osaka, T., Liu, X., Nojima, M., & Momma, T. (1999). An electrochemical double layer capacitor using an activated carbon electrode with gel electrolyte binder. *J. Electrochem. Soc., 146*(5), 1724–1729.

Portet, C., Taberna, P. L., Simon, P., Flahaut, E., & Laberty-Robert, C. (2005). High power density electrodes for carbon supercapacitor applications. *Electrocimica Acta, 50*, 4174–4181.

Rehbein, N., & Cooray, V. (2001). NOx production in spark and corona discharges. *J. Electrostat., 51–52*, 333–339.

White, H. J. (1963). *Industrial electrostatic precipitation*. Reading, Massachusetts: Addison-Wesley Publishing Co. Inc., pp. 1–87.

Xiang, X., Chen, B., & Colbeck, I. (2001). Bipolar charged aerosol agglomeration and collection by a two zone agglomerator. *J of Environmental Science, 13*(3), 276–279.

Yamamoto, T., & Velkoff, H. R. (1981). Electrohydrodynamics in an electrostatic precipitator. *J. Fluid Mech., 108*, 1–18.

Zou, L., Morris, G., & Qi, D. (2008). Using activated carbon electrode in electrosorptive deionization of brackish water. *Desalination, 225*, 329–340.